

No.	K22-3068	
Project Title	Programmed cell death induced by human coronavirus infection	
Principal Investigator	Kensuke Hirasawa (Memorial University of Newfoundland · Professor)	
Project Member(s)	IMSUT Host Researcher	Yasushi Kawaguchi (The Institute of Medical Science, The University of Tokyo · Professor)
	Project Member (s)	Yasushi Kawaguchi (Division of Molecular Virology, Department of Microbiology and Immunology · Professor)
	Project Member (s)	Jin Gohoda (Research Centre for Asian Infectious Disease · Associate Professor)
	Project Member (s)	Shinobu Kitazume (Department of Clinical Laboratory Sciences, School of Health Sciences, Fukushima Medical University · Professor)
	Project Member (s)	Kensuke Hirasawa (Division of BioMedical Sciences, Faculty of Medicine, Memorial University of Newfoundland · Professor)
	Project Member (s)	Lingyan Wang (Division of BioMedical Sciences, Faculty of Medicine, Memorial University of Newfoundland · PhD student)
	Project Member (s)	Joseph Duncan (Division of BioMedical Sciences, Faculty of Medicine, Memorial University of Newfoundland · PhD student)
	Project Member (s)	Maria Licursi (Division of BioMedical Sciences, Faculty of Medicine, Memorial University of Newfoundland · Postdoctoral Fellow)

IMSUT International Joint Usage/Research Center Project <International>

Joint Research Report (Annual/Project Completion)

Annual Report

Report

Project Outline**Project 1) Roles of programmed cell death in human coronavirus infection**

Programmed cell death (PCD) induced during virus infection results in inhibition of viral replication for certain viruses, but in promotion of it for other viruses. Until now, it remains to be studied what PCD can be induced during human coronavirus infection and how PCD impact replication of human coronaviruses. The Hirasawa lab at Memorial University recently identified that infection of non-pathogenic human coronaviruses (229E and OC43) induces pyroptosis and necroptosis, which, in turn, promotes their replication. To expand this study to SARS-CoV-2, the collaboration with Dr. Kawaguchi and Gohda at the Institute of Medical Sciences, supported by the IMSUT Joint research grant, has been established. Dr. Yasushi Kawaguchi, Dr. Jin Gohda, Dr. Ken Hirasawa, Dr. Maria Licursi and Lingyan Wang (PhD student) were involved in the project.

Project 2) Characterization of antiviral functions of interferon regulatory factors (IRFs) against human coronavirus infection

Human coronaviruses are known to be generally sensitive to antiviral actions of interferons. However, the functions of antiviral IRFs such as IRF1, IRF3 and IRF7 during human coronavirus infection have not been clarified. At Memorial University of Newfoundland, we determined antiviral functions of IRF1, IRF3 and IRF7 against human coronavirus 229E and OC43 (BSL2 level) and found that IRF3 is the most effective IRF against human coronavirus infection. With the collaboration with Dr. Kawaguchi and Gohda at the Institute of Medical Sciences, supported by the IMSUT Joint research grant, we also analyzed activation of the antiviral IRFs in SARS-CoV-2 infected cells. Dr. Yasushi Kawaguchi, Dr. Jin Gohda, Dr. Ken Hirasawa, Dr. Maria Licursi and Joseph Duncan (PhD student) were involved in the project.

Research Progress (April 2023-March 2023)

Project 1) Protein samples of SARS-CoV-2 infected cells were prepared at the BSL3 facility in at the Institute of Medical Sciences has been established, which were sent to Dr. Hirasawa's lab at Memorial University of Newfoundland. We conducted biochemical analysis and found that SARS-CoV-2 infection induces pyroptosis and necroptosis. A manuscript with the results is currently in preparation.

Project 2) The protein samples were analyzed for activation of interferon regulatory factors (IRFs) during SARS-CoV-2 infection. We identify that antiviral IRFs such as IRF1, 3 and 7 are activated during SARS-CoV-2 infection. This work was presented at the Canadian Society for Virology, at University of Alberta on June 6 2022 and accepted in *Frontiers in Immunology* (attached)

Dr. Hirasawa visited Dr. Kawguchi and Gohda at the Institute of Medical sciences, University of Tokyo on October 28, 2022 and discussed the research progress.

Dr. Hirasawa laboratory (Dr. Ken Hirasawa, Dr. Maria Licursi, Lingyan Wang, Joseph Duncan and Noah Conohan) participated the Joint Seminar in Virology held at the Institute of Medical sciences, University of Tokyo on March 9, 2023 and presented their research progress (attached).

Online meetings and email exchanges have been routinely held to maintain active collaboration and to plan further experiments.


Overall, we had a very good start of the collaboration between the two laboratories and are poised to expand our collaboration further next year.

Author's Proof

Before checking your proof, **please read the instructions below**

- Carefully read the entire proof and mark all corrections in the appropriate place, using the Adobe Reader commenting tools (**Adobe Help**). Do not use the Edit tool, as direct edits to the text will be ignored; annotate your corrections instead.
- Provide your corrections in a single PDF file or post your comments in the Production Forum making sure to reference the relevant query/line number. Upload or post all your corrections directly in the Production Forum to avoid any comments being missed.
- We do not accept corrections via email or in the form of edited manuscripts.
- Do not provide scanned or handwritten corrections.
- Before you submit your corrections, please make sure that you have checked your proof carefully as once you approve it, you won't be able to make any further corrections.
- To ensure timely publication of your article, please submit your corrections within 48 hours. We will inform you if we need anything else; do not contact us to confirm receipt.





Do you need help? Visit our **Production Help Center** for more information. If you can't find an answer to your question, contact your Production team directly by posting in the Production Forum.











NOTE FOR CHINESE-SPEAKING AUTHORS: If you'd like to see a Chinese translation, click on the  symbol next to each query. **Only respond in English** as non-English responses will not be considered. Translated instructions for providing corrections can be found [here](#).

Quick checklist

- Author names** - Complete, accurate and consistent with your previous publications.
- Affiliations** - Complete and accurate. Follow this style when applicable: Department, Institute, University, City, Country.
- Tables** - Make sure the meaning/alignment of your Tables is correct with the applied formatting style.
- Figures** - Make sure we are using the latest versions.
- Funding and Acknowledgments** - List all relevant funders and acknowledgments.
- Conflict of interest** - Ensure any relevant conflicts are declared.
- Supplementary files** - Ensure the latest files are published and that no line numbers and tracked changes are visible.
Also, the supplementary files should be cited in the article body text.
- Queries** - You must reply to **all of the typesetter's queries below** in order for production to proceed.
- Content** - Read all content carefully and ensure any necessary corrections are made, then **upload them** to the Production Forum.

Author queries form

Query no.	Details required	Authors response
Q1	Confirm whether the article title is correct. 	
Q2	Check that the amendments made to the title are satisfactory. 	
Q3	The citation and surnames of all of the authors have been highlighted. Check that they are correct and consistent with your previous publications, and correct them if needed. Please note that this may affect the indexing of your article in repositories such as PubMed. If adding/removing authors, or changing the order of this list, please provide us with a signed Authorship Change form 	
Q4	Confirm that the email address in your correspondence section is accurate. Any changes to corresponding authors requires individual confirmation from all original and added/removed corresponding authors. 	

Q5	We noticed a discrepancy between the author list in the submission system and the accepted manuscript (for authors Michael A. Joyce, Holly A. Saffran, Kaiwen Liu, Lorne D. Tyrrell). If adding/removing authors, or changing the order of this list, please provide us with a signed Authorship Change Form . You must complete and sign this form, then upload the file as a "Related Article" file type with your Author's Proof Corrections. 	
Q6	Confirm that all author affiliations are correctly listed. Per our style guidelines, affiliations are listed sequentially and follow author order. Requests for non-sequential affiliation listing will not be fulfilled. Note that affiliations should reflect those at the time during which the work was undertaken. If adding new affiliations, specify if these should be listed as a present address instead of a regular affiliation. 	
Q7	Provide the country details for Affiliation 4 and 6.	
Q8	The abstract should ideally be structured according to the IMRaD format (Introduction, Methods, Results and Discussion). Provide a structured abstract if possible. 	
Q9	Confirm that the keywords are correct, and keep them to a maximum of eight and a minimum of five. (Note: A keyword can be made up of one or more words.) 	
Q10	Reduce the number of keywords to a maximum of eight and a minimum of five. (Note: A keyword can be made up of one or more words.) 	
Q11	Check if the section headers (i.e., section leveling) have been correctly captured. 	
Q12	If you decide to use previously published and/or copyrighted figures in your article, please keep in mind that it is your responsibility as the author to obtain the appropriate permissions and licenses to reproduce them, and to follow any citation instructions requested by third-party rights holders. If obtaining the reproduction rights involves the payment of a fee, these charges are to be paid by the authors. 	
Q13	Check that all equations and special characters are displayed correctly. 	
Q14	If the following authors would like their LOOP profile to be linked to the final published version, ensure that they register with Frontiers at the provided link, and provide us with the URLs to their profile(s). Non-registered authors and authors with profiles set to "Private" will have the default profile image displayed. Note that we will not be able to add profile links after publication. "Joseph K. Sampson Duncan" "Michael A. Joyce" "Holly A. Saffran""Kaiwen Liu" "Jin Gohda" "Lorne D. Tyrrell" "Yasushi Kawaguchi"	
Q15	Ensure that all the figures, tables, and captions are correct, and that all figures are of the highest quality/resolution. If necessary, you may upload improved figures to the Production Forum. Please note that figures and tables must be cited sequentially, per the author guidelines 	
Q16	Ensure all grant numbers and funding information are included and accurate (after publication it is not possible to change this information). All funders should be credited, and all grant numbers should be correctly included in this section. 	

Q17	Confirm if the text included in the Conflict of Interest statement is correct. Please do not suggest edits to the wording of the final sentence, as this is standard for Frontiers' journal style. 🌐	
Q18	Confirm that the Data Availability statement is accurate. Note that this statement may have been amended to adhere to our Publication Ethics guidelines. 🌐	
Q19	Ensure that any supplementary material is correctly published at this link: https://www.frontiersin.org/articles/10.3389/fimmu.2023.930086/full#supplementary-material If the link does not work, you can check the file(s) directly in the production forum; the published supplementary files appear in green. Please make sure all Supplementary files are cited. Please also provide captions for these files, if relevant. If you have any corrections, please provide new files and republish them in the forum. Frontiers will deposit ALL supplementary files to FigShare and they will receive a DOI. Notify us of any previously deposited material. If the Supplementary Material files contain identifiable or copyright images, please keep in mind that it is your responsibility, as the author, to ensure you have permission to use the images in the article. Please check this link for information on author responsibilities and the publication images. 🌐	
Q20	Confirm that the details in the "Author Contributions" section are correct. We have added the sentence "All authors contributed to the article and approved the submitted version." 🌐	
Q21	Please confirm if this should be moved to a Funding section: "This work was supported by grants from the Canadian Institutes for Health Research (CIHR) (KH), the Natural Sciences and Engineering Research Council of Canada (NSERC) (KH), the Japan Agency for Medical Research and Development (AMED) (Grant Number JP20wm0125002) (YK and JG), a grant from the international Joint Research Project of the Institute of Medical Science, the University of Tokyo and Memorial University of Newfoundland (KH). DX was supported by the Dean's fellowship from Faculty of Medicine, Memorial University of Newfoundland."	
Q22	Provide the page range for the following references, if applicable. 25, 28, 41, 43, 68. 🌐	
Q23	Please provide the doi for "21; 40; 61; 70", if applicable. 🌐	
Q24	We received the Supplementary Material inside the manuscript. Please provide this as a separate supplementary file. 🌐	
Q25	Note that Affiliation 2-6 were interchanged since their citations need to be listed in sequential order, per our style. If they need to be switched back, please move the citations into sequential order. 🌐	
Q26	The image used in Figure 1 does not have any symbols "***" and "*****"; however, these symbol symbols "***" and "*****" were present in the caption. Could you clarify this? Provide revised files if necessary. 🌐	
Q27	Provide the meaning of symbol "****" provided in Figure 2. 🌐	
Q28	Provide the meaning of symbol "**" provided in Figure 6. 🌐	



OPEN ACCESS

EDITED BY
Kathrin Sutter,
University of Duisburg-Essen, Germany

REVIEWED BY
Pin Ling,
National Cheng Kung University, Taiwan
Vu Thuy Khanh Le-Trilling,
Essen University Hospital, Germany

Q4 *CORRESPONDENCE
Kensuke Hirasawa
✉ kensuke@mun.ca

[†]These authors have contributed equally to this work

SPECIALTY SECTION
This article was submitted to
Viral Immunology,
a section of the journal
Frontiers in Immunology

RECEIVED 27 April 2022
ACCEPTED 27 March 2023
PUBLISHED xx xx 2023

CITATION
Duncan JKS, Xu D, Licursi M, Joyce MA,
Saffran HA, Liu K, Gohda J, Tyrrell LD,
Kawaguchi Y and Hirasawa K (2023)
Interferon regulatory factor 3 mediates
effective antiviral responses to human
coronavirus 229E and OC43 infection.
Front. Immunol. 14:930086.
doi: 10.3389/fimmu.2023.930086

COPYRIGHT
© 2023 Duncan, Xu, Licursi, Joyce, Saffran,
Liu, Gohda, Tyrrell, Kawaguchi and Hirasawa.
This is an open-access article distributed
under the terms of the [Creative Commons
Attribution License \(CC BY\)](#). The use,
distribution or reproduction in other
forums is permitted, provided the original
author(s) and the copyright owner(s) are
credited and that the original publication in
this journal is cited, in accordance with
accepted academic practice. No use,
distribution or reproduction is permitted
which does not comply with these terms.

Interferon regulatory factor 3 mediates effective antiviral responses to human coronavirus 229E and OC43 infection

Joseph K. Sampson **Duncan**^{1†}, Danyang **Xu**^{1†}, Maria **Licursi**¹,
Michael A. **Joyce**^{2,3}, Holly A. **Saffran**^{2,3}, Kaiwen **Liu**¹, Jin **Gohda**⁴,
Lorne D. **Tyrrell**^{2,3}, Yasushi **Kawaguchi**^{4,5,6}
and Kensuke **Hirasawa**^{1*}

¹Division of BioMedical Sciences, Faculty of Medicine, Memorial University of Newfoundland, St. John's, NL, Canada, ²Li Ka Shing Institute of Virology, University of Alberta, Edmonton, AB, Canada, ³Department of Biochemistry, University of Alberta, Edmonton, AB, Canada, ⁴Research Center for Asian Infectious diseases, The Institute of Medical Science, The University of Tokyo, ⁵Division of Molecular Virology, Department of Microbiology and Immunology, The Institute of Medical Science, The University of Tokyo, Tokyo, Japan, ⁶Department of Infectious Disease Control, International Research Center for Infectious Diseases, The Institute of Medical Science, The University of Tokyo

Interferon regulatory factors (IRFs) are key elements of antiviral innate responses that regulate the transcription of interferons (IFNs) and IFN-stimulated genes (ISGs). While the sensitivity of human coronaviruses to IFNs has been characterized, antiviral roles of IRFs during human coronavirus infection are not fully understood. Type I or II IFN treatment protected MRC5 cells from human coronavirus 229E infection, but not OC43. Cells infected with 229E or OC43 upregulated ISGs, indicating that antiviral transcription is not suppressed. Antiviral IRFs, IRF1, IRF3 and IRF7, were activated in cells infected with 229E, OC43 or severe acute respiratory syndrome-associated coronavirus 2 (SARS-CoV-2). RNAi knockdown and overexpression of IRFs demonstrated that IRF1 and IRF3 have antiviral properties against OC43, while IRF3 and IRF7 are effective in restricting 229E infection. IRF3 activation effectively promotes transcription of antiviral genes during OC43 or 229E infection. Our study suggests that IRFs may be effective antiviral regulators against human coronavirus infection.

KEYWORDS

SARS-CoV2, OC43, 229E, innate immunity, interferon, interferon stimulate genes, IRF1, IRF3, IRF7

Introduction

Human coronaviruses are enveloped single-stranded RNA viruses with positive-sense genomes that commonly cause respiratory tract infection in humans (1, 2). They are comprised of 4 genera: alphacoronavirus, betacoronavirus, gammacoronavirus, and deltacoronavirus. Certain betacoronaviruses are known to cause lethal infection in

humans, including middle east respiratory syndrome (MERS), severe acute respiratory syndrome-associated coronavirus (SARS-CoV) and SARS-CoV-2. MERS infection was first found in 2012; since then, 2249 infections and 858 deaths in 27 countries have been reported (3). SARS-CoV caused 8237 infections and 775 deaths in more than 30 countries in 2002 (4). SARS-CoV-2 was identified in 2019 and is responsible for the current COVID-19 pandemic. As of today (March 1, 2023), 679 million cases and 6.8 million deaths have been reported worldwide (5). Other human coronaviruses, such as OC43, 229E, NL63 and HKU1, infect the upper respiratory tract and cause common seasonal cold symptoms (6). OC43 and HKU1 are members of the genera betacoronaviruses, while 229E and NL63 are alphacoronaviruses (7, 8). As the sequence of non-structural proteins are well-conserved among human coronaviruses, they share very similar replication cycles (9, 10).

Cells sense viral products intracellularly and extracellularly using different pattern recognition receptors (PRRs) such as toll-like receptors, RIG-I-like receptors and melanoma differentiation-associated gene 5 (MDA-5) (11). The recognition of viral products results in activation and nuclear translocation of IFN regulatory factor 3 (IRF3), IFN regulatory factor 7 (IRF7) and nuclear factor- κ B (NF- κ B), which activate the transcription of interferons (IFNs) (12, 13). IFNs, which have three classes, type I (IFN- α/β), type II (IFN- γ) and type III (IFN- λ) IFNs, play essential roles in antiviral innate immune response (14, 15). Secreted IFNs bind to IFN receptors in an autocrine or paracrine manner and activate the Janus kinase (JAK)-signal transducer and activator of transcription (STAT) (16, 17). Phosphorylated STAT proteins along with other transcriptional regulators such as IRF1 and IRF9 directly bind to the promoter regions of IFN-stimulated genes (ISGs) to activate their transcription (18, 19). Human coronaviruses are generally sensitive to antiviral functions of IFNs albeit with some differences in their sensitivity. Both SARS-CoV and MERS are sensitive to IFN when cells are treated at high concentrations (20–23). Between the two viruses, IFNs are more effective in inhibiting the replication of MERS than SARS-CoV (23). Moreover, SARS-CoV-2 is more sensitive to type I IFNs than SARS-CoV (24, 25). As for other human coronaviruses, IFNs suppress OC43 infection in a cell type dependent manner (26), while 229E is sensitive to IFN treatment *in vitro* (20, 27). These reports suggest that human coronaviruses are generally sensitive to IFNs, but each virus has different levels of sensitivity.

In clinical settings, IFN- β treatment significantly reduced the mortality of SARS-CoV-2 infected patients when administrated at an early stage of infection (28). Similarly, treatment of pegylated IFN- α significantly reduced viral replication of SARS-CoV in macaques (29). In STAT1 $-/-$ mice, SARS-CoV induced a prolonged infection with higher viral loads in the lung, suggesting that the JAK/STAT pathway downstream of IFN receptors is essential for clearing SARS-CoV *in vivo* (30). However, SARS-CoV infection was not exacerbated in IFN- α/β receptor $-/-$ mice, but instead mouse survival was improved due to reduced immune cell infiltration in the lung, indicating immunopathogenic roles of IFNs in SARS-CoV infection (31).

While the antiviral efficacy of IFNs against human coronavirus is clear, SARS-CoV-2 infected patients displayed low production of type

I and III IFN and a moderate ISG response (32). Similarly, type I IFN response was delayed in mice infected with SARS-CoV-2, allowing viral replication, lung immunopathogenesis and lethal pneumonia (31). These reports suggest that IFN-mediated antiviral innate responses are dysregulated in SARS-CoV-2 infection *in vivo*. This is most likely due to the presence of SARS-CoV-2 proteins that suppress the production of IFNs and ISGs (33). In summary, IFNs have antiviral and immunopathogenic roles in human coronavirus infection. Moreover, IFN antiviral responses are targets of immune evasion mechanisms by human coronaviruses.

Among IRFs, IRF1, IRF3, and IRF7 are transcriptional regulators of IFNs and ISGs (34, 35). IRF1 is upregulated during viral infection or IFN stimulation, which, in turn, activates transcription of type I IFNs (36, 37). As IRF1 is a co-transcriptional factor of ISGs regulated by the Jak/STAT pathway, a subset of ISGs can be induced by IRF1 in an IFN-independent manner (38). Upon virus infection, the innate immune sensors interact with viral components and activate the TANK-binding Kinase 1 (TBK1)/ κ B kinase ϵ (IKK ϵ) complex, which induces the activation of both IRF3 and IRF7 (39, 40). The activation of IRF3 and IRF7 results in the translocation of these proteins to the nucleus where they initiate the transcription of type I IFNs. Similar to IRF1, IRF3 can also exhibit antiviral functions independently of the IFN system by upregulating ISGs independently of IFN production *in vitro* (41, 42). IRF3 could be an important component of innate immune responses against SARS-CoV-2, as blocking phosphorylation and translocation of IRF3 promotes its replication (43). Accumulating evidence suggests that human coronaviruses can interfere with the activity of IRF3. SARS-CoV-2 PLpro and 3CLpro, viral proteins responsible for cleaving viral polyproteins, also degrade IRF3 (44, 45). Other studies demonstrated that SARS-CoV-2 7a reduces IRF3 phosphorylation by downregulating TBK1 expression levels (46, 47). Similarly, SARS-CoV 8b and 8ab induce IRF3 degradation in a ubiquitin dependent manner (44), while MERS M protein disrupts the interaction of TNF Receptor Associated Factor 3 (TRAF3) and TBK1, leading to reduced IRF3 activation (44). These studies clearly suggest that human coronavirus proteins target IRF3 to promote their replication. In contrast to IRF3, antiviral roles of IRF1 and IRF7 against human coronavirus infection are less understood. In animal coronaviruses, IRF1 was shown to have antiviral properties against mouse hepatitis virus (MHV) (48). The viral M protein of porcine epidemic diarrhea virus (PEDV) interacts with IRF7 and inhibits its antiviral functions (33, 49). Thus, it is possible that IRF1 and IRF7 also have antiviral effects in human coronavirus infection.

Although it is suggested that the antiviral IRFs are important for host antiviral responses against human coronavirus infection, there is no direct functional evidence reported. In this study, we conducted loss- and gain-of-function experiments of IRF1, IRF3 and IRF7 to clarify antiviral functions of IRF1, IRF3 and IRF7 during human coronavirus infection. To fight against human coronavirus infection, it is important to gain more knowledge about antiviral responses mediated by IRFs during human coronavirus infection.

Materials and methods

Cells, viruses, and reagents

Human lung fibroblast cell line MRC5, human lung cancer cell line H1299, monkey kidney epithelial cell line Vero E6, mouse fibroblast cell line L929, human coronaviruses HCoV-OC43 and HCoV-229E were obtained from the American Type Culture Collection (ATCC; Manassas, VA, USA). Human dermal fibroblast cells were obtained from Cell Applications Inc. (San Diego, CA, USA). Vesicular stomatitis virus (VSV, Indiana strain) was provided by Dr. John C. Bell (Centre for Innovative Cancer Therapeutics, Ottawa Hospital Research Institute, Ottawa, Canada). VSV was amplified and titrated by plaque assay using L929 cells as described previously (50). SARS-CoV-2 (SARS-CoV-2/CANADA/VIDO/01/2020) was isolated at the VIDO, University of Saskatchewan from a clinical specimen obtained at the Sunnybrook Health Sciences Centre, and propagated at the National Microbiology Laboratory (NML) was amplified and titrated by plaque assay using Vero E6 cells (51). Recombinant human IFN- α A, human IFN- γ and IFN- λ 1 were obtained from Bio-Rad, BD Pharmingen and R&D Systems respectively. Antibodies used in this study include: IRF3, phospho-IRF3, IRF7, phospho-STAT1 (Cell signalling technology), IRF3 (Santa Cruz), IRF1 (BD Transduction Laboratories), GAPDH (Santa Cruz Biotechnology), 229E N protein (Ingenasa), OC43 N protein (Millipore), SARS-CoV-2 spike protein (Sino Biological). Negative control siRNA, IRF1 siRNA (s7501), IRF3 siRNAs (s7509) and IRF7 siRNA (s223948) were purchased from Life Technologies. IRF1-pINCY plasmid (Open biosystems) and IRF7 -ORF vector (Applied Biological Materials) was subcloned into pcDNA3 plasmid (Addgene). pcDNA3-IRF3 was purchased from Addgene.

Cell culture

All cells were cultured in high-glucose Dulbecco's modified Eagle's medium (Corning, MA) supplemented with 10% fetal bovine serum (HyClone, Cytiva), 1 mM sodium pyruvate (Life Technologies) and antibiotic-antimycotic (Thermo Scientific). Cells were maintained in 10-cm culture dishes at 37°C with 5% CO₂ for the use of experiments in this work. Human Dermal Fibroblasts were grown on dishes coated with 0.1% gelatine (from Cell Applications, Inc).

Virus infection

Cells with 90% confluency were infected with human coronavirus 229E or OC43 with a MOI of 0.01. The diluted stock viruses were adsorbed for 2 hours at 33°C, and then removed and replaced with DMEM with 2% FBS. Infected cells were incubated at 33°C with 5% CO₂ for up to six days. For IFN treatment, MRC5 cells were treated with IFN- α (250 and 500 U/ml), IFN- γ (50 and 100 U/ml) or left untreated for 18 hours and then challenged with

229E or OC43. For siRNA knockdown, cells were transfected with 5 pmol siRNA oligos using Lipofectamine RNAiMAX Transfection Reagent (Life Technologies) and 24 hours later challenged with or without 229E or OC43 (MOI of 0.01). For overexpression of IRFs, cells in 24-well plates (4×10^4 cells/well) were transfected with control pcDNA3, pcDNA-IRF1, pcDNA-IRF3 or pcDNA-IRF7 using Lipofectamine 3000 Transfection Reagent (Life Technologies) and 24 hours later challenged with or without 229E or OC43. VSV absorption and infection (MOI of 0.0001) were conducted at 37°C with 5% CO₂. The amount of progeny viruses in the culture supernatant was measured by TCID50 (50% tissue culture infective dose) assay for 229E and OC43 (52) and plaque assay for VSV (50).

Vero E6 cells expressing TMPRSS2 were seeded into 12 well plates and infected with SARS CoV-2 at MOI 0.01 or 0.1 and absorbed for 1 hour at 37°C in DMEM with 2% FBS. After absorption period, virus was aspirated and replaced with DMEM containing 5% FBS. At 8 or 24 hours post infection (hpi), cells were washed with PBS and harvested with RIPA buffer. All infections were performed in the Canada Foundation for Innovation Containment Level 3 Facility at the University of Alberta.

UV-inactivation of OC43 and 229E was performed by diluting the virus in 4ml DMEM with 2% FBS and placed in a 6 cm plastic petri dish at 45 cm from a 60 W ultraviolet tube for 10 min (53).

Western blot analysis

Cells in each well of a 24-well plate were harvested with 100 μ l radioimmunoprecipitation assay (RIPA) buffer supplemented with protease inhibitors (Sigma-Aldrich) and phosphatase inhibitors (Thermo Scientific). SDS sample buffer was added to cell lysates, followed by a 5-minute boiling period. The same volume of each sample was subjected to 10% SDS-PAGE. To use the housekeeping protein (GAPDH) as an indicator of infection/cell death in the experiments, the loading amounts of the samples were not adjusted by protein assay. The proteins were then transferred to nitrocellulose membranes (Bio-Rad, ON, Canada) using a Trans-blot Turbo Transfer System (Bio-Rad). The membrane was blocked with 5% skim milk in tris-buffered saline (TBS) with 0.1% Tween 20 (TBS-T) for 1 hour at room temperature and then incubated with primary antibodies overnight at 4°C. The following day, membranes were incubated with peroxide-conjugated anti-rabbit or anti-mouse secondary antibody (Santa Cruz Biotechnology) for 1 hour. Specific bands were detected with ImageQuant LAS 4000 (GE Healthcare Life Sciences, QC, Canada) using enhanced chemiluminescence western blotting detection reagent (Bio-Rad or Amersham).

Quantitative RT-PCR

Quantitative RT-PCR (RT-qPCR) was performed in triplicate using the previously described validation strategies (54). RNA was isolated from MRC5 and H1299 cells using TRIzol (Invitrogen) according to the manufacturer's instructions. cDNA was synthesized from the RNA using the RevertAid H Minus First

Strand cDNA Synthesis Kit (Thermo Scientific). Quantitative PCR (qPCR) was performed in triplicates using powerSYBR[®]Green PCR Master Mix (Life Technologies LTD, UK) and analyzed with StepOnePlus qPCR system (Applied Biosystems, CA). The polymerase chain reaction (PCR) procedure was as manufacturer's instructions: 95°C for 10 minutes followed by 40 cycles of 95°C for 15 seconds, 60°C for 1 minute, and then followed by melt-curve analysis. For data analysis, mRNA levels of each gene were normalized to GAPDH. The fold change of each sample toward the parental cells sample was calculated using the $2^{-\Delta\Delta CT}$ method. The experiment was conducted with biological triplicates. The primer sequences are shown in [Supplementary Table 1](#). A five-point, five-fold dilution series was used for primer validation.

Statistical analysis

One-way ANOVA and two-way ANOVA with Dunnett's or Turkey's *post-hoc* test were performed using GraphPad Prism 6.0 software.

Results

IFN treatment delays 229E infection but not OC43 infection

To investigate the antiviral effects of IFNs on human coronavirus infection, we first tested if human lung fibroblast cells, MRC5, are sensitive to different types of IFNs ([Figure 1A](#)). When MRC5 cells were treated with IFN- α , IFN- γ or IFN-Lambda; for 30 mins, we observed STAT1 phosphorylation in cells treated with IFN- α or IFN- γ , but not in those treated with IFN-Lambda; This indicates that MRC5 cells are sensitive to type I and type II IFN, but not to type III IFN. MRC5 cells are reported to lack IFN-Lambda; receptor ([55](#), [56](#)). Therefore, we focused on type I and II IFN for the following experiments.

MRC5 cells were left untreated or treated with IFN- α (250 and 500 U/ml) or IFN- γ (50 and 100 IU/ml) for 18 hours and then challenged with 229E ([Figure 1B](#)) or OC43 ([Figure 1C](#)) at a MOI of 0.01. Cell lysates were harvested at 2, 4 and 6 days after infection for western blot analysis of viral nucleocapsid proteins N) and GAPDH. At 2 days following 229E infection, viral protein was detected in cells without IFN- α treatment, but not in cells treated with IFN- α ([Figure 1B](#)). At 4 days after infection, less viral protein was detected with a higher IFN- α concentration (500 IU/ml). Similarly, IFN- γ treatment inhibited 229E infection at 2 days, but not at 4 and 6 days after infection. In contrast, OC43 infection was not significantly affected by IFN- α or IFN- γ , although some minor reductions in viral protein levels were observed in cells treated with IFNs at 2 days after infection ([Figure 1C](#)). To further confirm the effect of IFNs on virus production, we conducted a progeny virus assay ([Figures 1D, E](#)). The amount of progeny 229E was significantly lower in cells treated with IFN- α or IFN- γ at 2 days after infection ([Figure 1D](#)). On the other hand, IFN treatment did not reduce the progeny virus production of OC43 ([Figure 1E](#)).

Similarly, OC43 infection was not sensitive to IFN treatment in human lung cancer cell line H1299, while 229E infection was inhibited ([Supplementary Figure 1](#)). To confirm the efficacy of IFN to induce sufficient antiviral responses, we conducted a positive control experiment where MRC5 cells were treated with the same amount of IFN- α or IFN- γ , and then challenged with an IFN-sensitive virus, vesicular stomatitis virus (VSV). The IFN treatment completely inhibited VSV protein synthesis ([Figure 1F](#)) and progeny virus production ([Figure 1G](#)), indicating the concentration of IFN used in our system is sufficient to inhibit the replication of an IFN-sensitive virus. At 4 days after VSV infection, the expression levels of GAPDH and VSV G were very low in infected cells without IFN treatment, indicating that VSV replication was not active because most cells were dead.

Taken together, these results suggest that both type I and II IFN delay 229E infection in MRC5 and H1299 cells, but they are not effective in protecting against OC43 infection.

229E and OC43 infection activate transcription of IFN-stimulated genes

Our next question was whether human coronaviruses activate antiviral innate responses in infected cells. To test this, we assessed the transcriptional activation of ISGs at 2 and 4 days after human coronavirus infection ([Figure 2](#)). Western blot analysis was first conducted to confirm infection of 229E ([Figure 2A](#)) and OC43 ([Figure 2B](#)). Then, the expression of the following IFN-inducible genes was examined during 229E ([Figure 2C](#)) or OC43 ([Figure 2D](#)) infection: guanylate binding protein 2 (GBP2) ([57](#)), interferon induced protein 44 (IFI44) ([58](#)), interferon induced protein with tetratricopeptide repeats 2 (IFIT2) ([59](#)), microtubule-associated protein 2 (MAP2) ([54](#)), retinoic acid-inducible gene I (RIG-I) ([60](#)) and STAT2 ([61](#)). 229E infection did not induce GBP2, but significantly increased the expression of all other genes at 4 days after infection. In contrast, OC43 infection induced all IFN-inducible genes tested at 2 days after infection, and the expression levels were significantly higher than control at 4 days except for GBP2 and STAT2. The expression of the ISGs was induced at the earlier stage of infection in cells infected with OC43 than those infected with 229E. The ISG induction was not observed in cells infected with UV-inactivated 229E or OC43 (MOI of 0.01), suggesting that active infection is required for the ISG induction ([Supplementary Figure 2](#)). While GBP2 induction in MRC5 cells infected with 229E or OC43C infection was lower than those stimulated with IFN- γ , the expression levels of RIG-I and STAT2 induced by 229E or OC43 infection were similar to those induced by IFN- α or - γ stimulation ([Supplementary Figure 2](#)). These results demonstrate that human coronavirus infection induces host antiviral transcriptional responses.

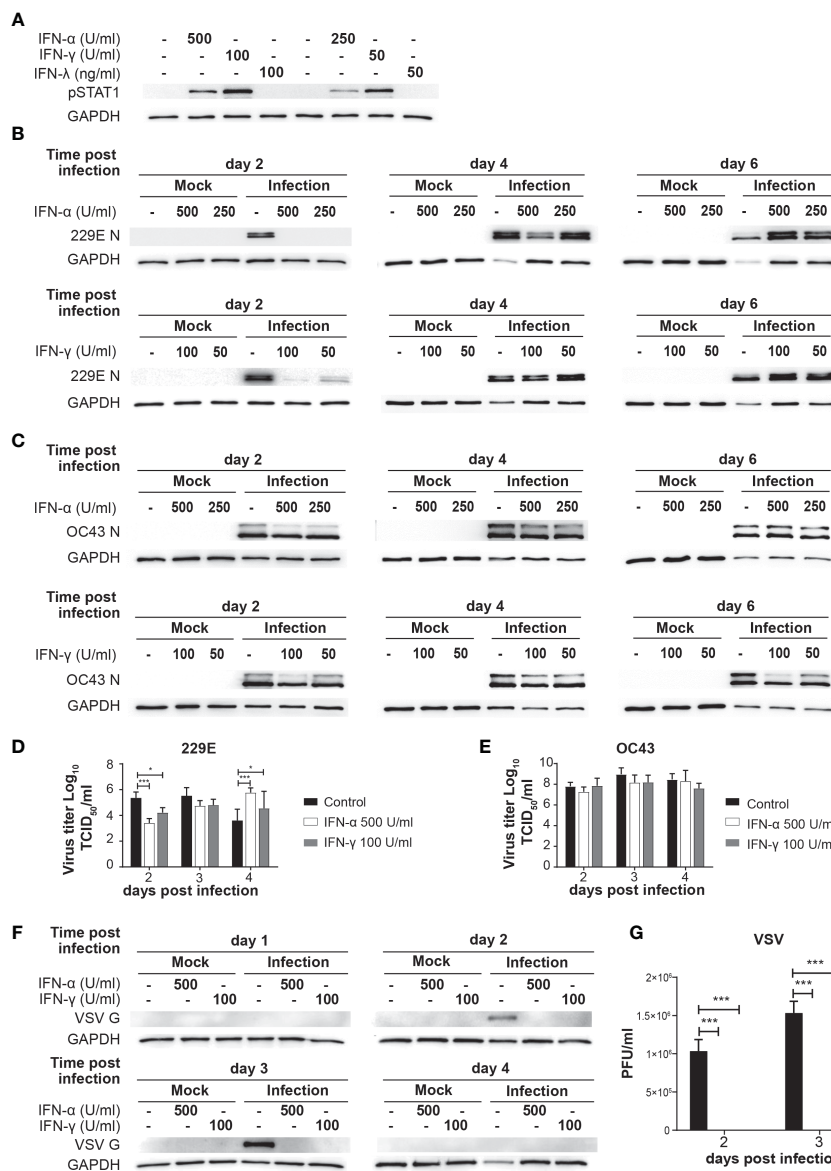


FIGURE 1

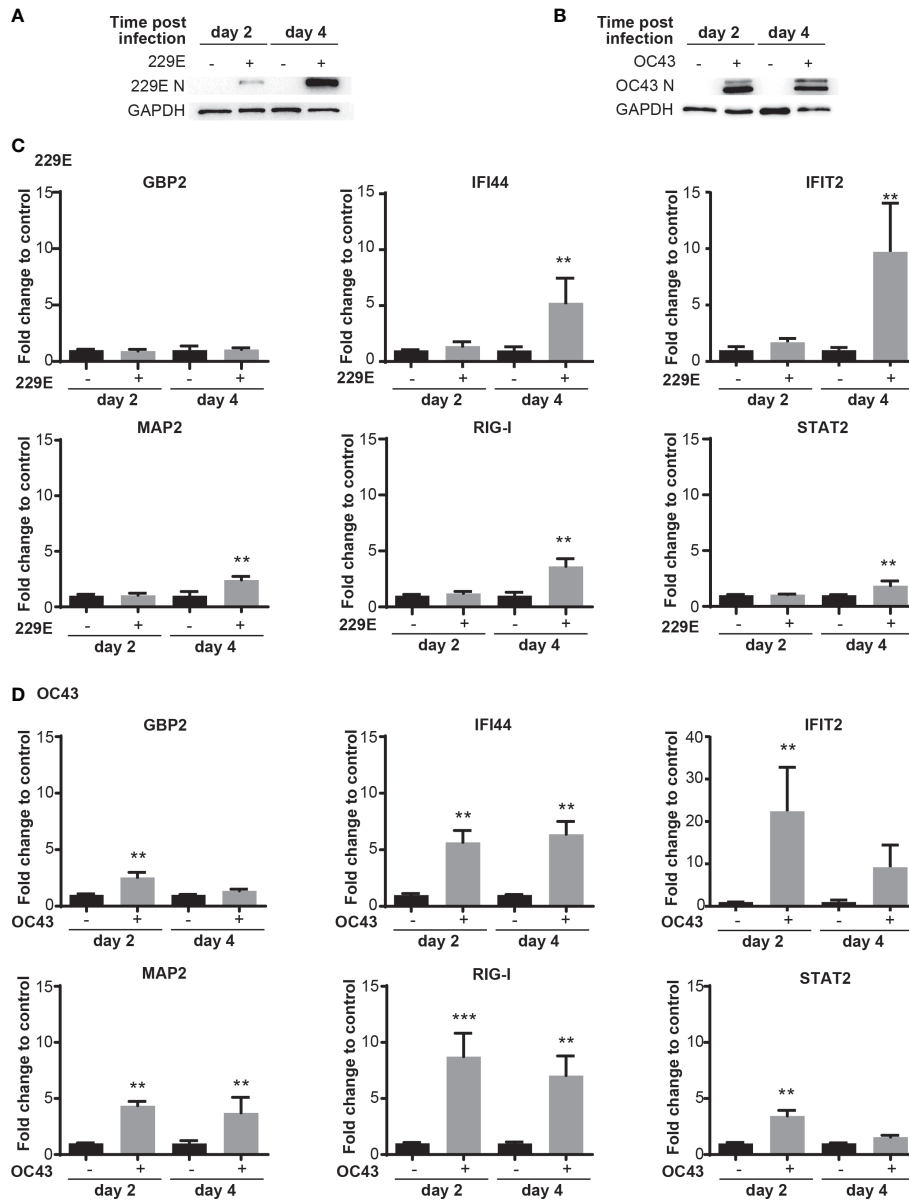
IFN treatment delays 229E but not OC43 infection. (A) MRC5 cells were left untreated or treated with IFN- α (500 and 250 U/ml), IFN- γ (100 and 50 U/ml) or IFN- λ (100 and 50 ng/ml) for 30 min. STAT1 activation was determined by western blot analysis using anti phospho-STAT1 and GAPDH antibodies. (B and C) MRC5 cells were left untreated or treated with IFN- α or IFN- γ for 18 hours, and then challenged with 229E (B) or OC43 (C) infection at MOI of 0.01. Western blot analysis of viral protein was conducted using anti 229E N protein (B), OC43 N protein (C) and GAPDH antibodies. (D, E) TCID₅₀ assay was performed to measure the progeny virus of 229E or OC43 infected MRC5 cells left untreated or treated with IFNs (n=3). (F, G) MRC5 cells were left untreated or treated with IFN- α (500U/ml) or IFN- γ (100U/ml), and then challenged with VSV at MOI of 0.0001. VSV infection was determined by (F) western blot analysis using anti VSV G and GAPDH antibodies and (G) plaque assay using L929 cells (n=3). The amount of progeny virus is shown as plaque forming units (PFU)/ml of samples nontreated or treated with IFN. *p<0.05, **p<0.01, ***p<0.001, ****p<0.0001, Two-way ANOVA.

Q12
Q15
Q26

IRF1, IRF3 and IRF7 are activated during human coronavirus infection

As IRF1, IRF3 and IRF7 are the key transcriptional regulators of IFNs and ISGs, we sought to determine their activation status during human coronavirus infection. Accordingly, a western blot analysis was conducted to assess the expression of IRF1 and IRF7, and phosphorylation of IRF3 (an active form of IRF3) in MRC5 cells infected with 229E or OC43. After 229E infection, viral proteins were detected from day 2 and reached a peak at day 3

and 4 (Figure 3A). The expression of IRF1 and IRF7 was increased at 3 and 4 days after infection compared to uninfected controls. Similarly, phosphorylated IRF3 increased at the same time points. After OC43 infection, OC43 nucleoprotein was detected at day 1, which peaked at 3 and 4 days after infection (Figure 3B). In these infected cells, IRF1 expression increased at day 2 and 3. We observed an upper shift in IRF1 bands, which could be caused by posttranslational modifications of IRF1. IRF3 and IRF7 were also activated from 2 to 5 days after OC43 infection. Activation of IRFs was not observed in cells infected with UV-inactivated 229E or



Q27

FIGURE 2 Human coronavirus infection activates transcription of IFN-stimulated genes. MRC5 cells were left uninfected or infected with 229E (A, C) or OC43 (B, D) at MOI of 0.01. Infection of 229E (A) and OC43 (B) was confirmed by western blot analysis using anti 229E N protein, OC43 N protein and GAPDH antibodies. The mRNA levels of ISGs (GBP2, IFI44, IFIT2, MAP2, RIG-I and STAT2) were determined by RT-qPCR in MRC5 cells infected with 229E (C) or OC43 (D) (n=6). The fold change to control indicates the fold change of the expression level for infected samples towards that of the non-infected controls at the same time point post infection. The transcriptional level for each gene was calculated by normalizing to GAPDH expression level and then normalized by the corresponding control. **p<0.01, Two-way ANOVA.

OC43 infection while IFN stimulation induces higher activation of the IRFs than 229E or OC43 infection (Supplementary Figure 3). We also confirmed the activation of IRF1 and IRF3 in human primary dermal cells (Supplementary Figure 4). The dermal cells supported 229E or OC43 infection, which increased IRF1 expression at day 2 and 3, and phosphorylation of IRF3 from day 2 to 5. However, activation of IRF7 was not observed.

To determine the effect of SARS-CoV-2 infection on IRFs, Vero E6 cells expressing TMPRSS2 were infected with SARS-CoV-2 at a MOI of 0.01 or 0.1 (Figure 3D). Viral proteins were detected at in cells infected with a MOI of 0.01 at 24 hours post-infection, and at 8

and 24 hours post-infection when infection at a MOI of 0.1. In SARS-CoV-2 infected cells, there was an increase in IRF1 and IRF7 expression and IRF3 phosphorylation, suggesting that SARS-CoV-2 infection also activates antiviral IRFs.

These results demonstrate that IRF1, IRF3 and IRF7 are activated during human coronavirus infection.

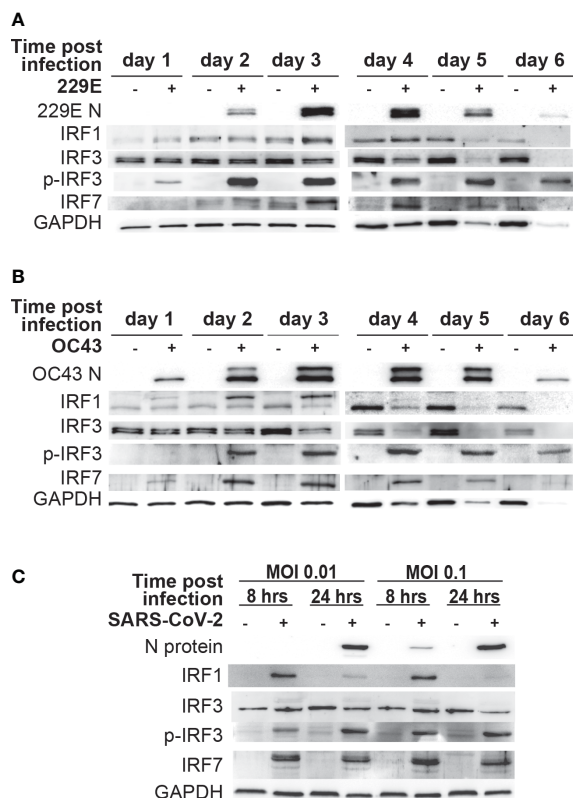


FIGURE 3

Human coronavirus infection activates IRF1, IRF3 and IRF7. MRC5 cells were left uninfected (-) or infected (+) with 229E (A) or OC43 (B) at MOI of 0.01. (C) Vero E6 cells expressing TMPRSS2 were left uninfected or infected with SARS-CoV-2 at MOI of 0.01 or at MOI 0.1. The activation of IRF1, IRF3 and IRF7 was determined by western blot analysis using antibodies against 229E N protein, OC43 N protein, SARS-CoV-2 N protein, IRF1, IRF3, IRF7, phosphorylated (p-IRF3) and GAPDH.

IRF1, 3 and 7 have antiviral roles against human coronavirus infection

To investigate the functional roles of IRF1, IRF3 and IRF7 during human coronavirus infection, we conducted a loss-of-function analysis using siRNA knockdown. MRC5 cells were transfected with either control siRNA oligos or those against IRF1, IRF3 or IRF7 for 24 hours. The knockdown of IRF1 and IRF3 was confirmed with western blot analysis, which showed lower expression levels in cells treated with their corresponding siRNA oligos (Figure 4A). As IRF7 expression is undetectable by western blot in non-infected cells, IRF7 knockdown was confirmed by qPCR analysis (Figure 4B). When these cells were challenged with 229E or OC43, RT-q-PCR analysis revealed that IRF1 knockdown promotes 229E infection at 3 days after infection and OC43 infection at 2 and 3 days after infection (Figure 4C). IRF3 knockdown also increased the expression of viral RNA at 2 and 3 days after 229E infection and 2 days after OC43 infection. In addition, IRF7 knockdown resulted in an increase in 229E infection at 3 days after infection and OC43 infection at 2 and 3 days after infection. These results were further confirmed by western blot analysis (Figure 4D). 229E viral protein synthesis was increased in cells treated with siRNA oligos against IRF3 or IRF7 compared to siRNA controls at 2 days after infection. For OC43 infection, knockdown of IRF1 or IRF3 promoted viral

protein synthesis compared to siRNA controls at both 2 and 3 days after infection. Altogether, these loss-of-function experiments indicate the antiviral roles of IRF1, IRF3 and IRF7 against coronavirus infection.

To further confirm the antiviral roles of IRF1, IRF3 and IRF7, we conducted gain-of-function experiments *via* overexpression. H1299 cells were transfected with control pcDNA3, IRF1-pcDNA3, IRF3-pcDNA3 or IRF7-pcDNA3 for 24 hours and then challenged with 229E or OC43 (Figure 5). IRF1 overexpression effectively inhibited replication of OC43 as the generation of viral proteins and progeny viruses were lower in cells transfected with IRF1-pcDNA than those transfected with control pcDNA3 (Figure 5A). We observed a slight reduction of 229E N protein expression in IRF1 overexpressed cells at 1 day after infection, but there was no significant difference in the amount of progeny virus (Figure 5D). Moreover, 229E and OC43 generated less viral proteins and progeny viruses in the cells transfected with IRF3-pcDNA3 (Figures 5B, E), suggesting that IRF3 introduction promoted antiviral activities against both 229E and OC43. Finally, the introduction of IRF7 effectively reduced 229E infection, but not OC43 infection, as shown in western blotting and progeny virus analysis (Figures 5C, F).

To clarify how IRFs demonstrate different antiviral effects against human coronavirus infection, we investigate expression

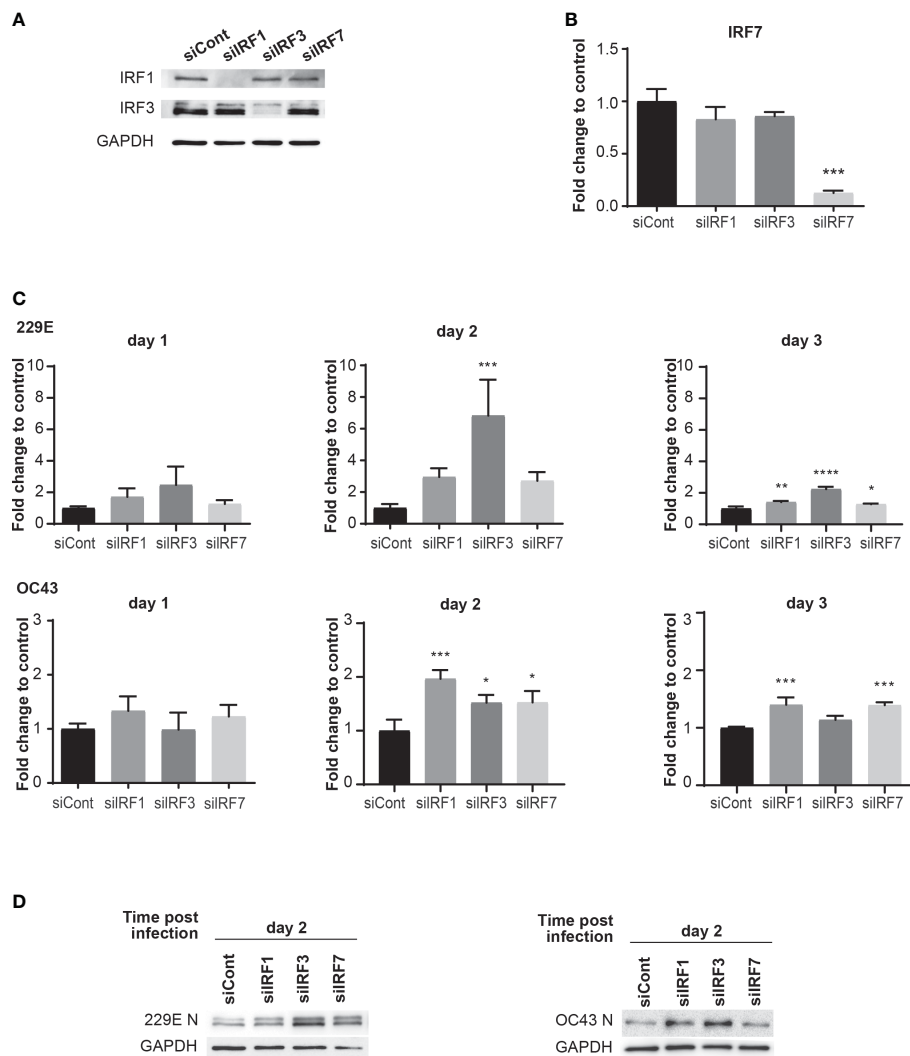


FIGURE 4

Knockdown of IRFs promotes human coronavirus infection. MRC5 cells were transfected with control siRNA (siCont), IRF1 siRNA, IRF3 siRNA or IRF7 siRNA oligoes (5 pmol) using Lipofectamine RNAiMAX transfection reagent. The knockdown of IRFs expression was confirmed by western blot analysis for IRF1 and IRF3 (A) and RT-qPCR for IRF7 (B). MRC5 cells were then infected with 229E or OC43 at MOI of 0.01. (C) The amounts of viral RNA were measured by RT-qPCR (n=3). (D) The amounts of viral protein were determined by western blot analysis using antibodies against 229E N protein, OC43 N protein and GAPDH. For RT-qPCR analysis, the transcription level for each gene was first normalized to GAPDH expression level. The fold change to control indicates the fold change of the expression level for IRFs siRNA transfected samples to that of the control siRNA transfected samples. * $p < 0.05$, ** $p < 0.01$, *** $p < 0.001$, **** $p < 0.0001$, Two-way ANOVA.

levels of antiviral genes in cells transfected with control pcDNA3, IRF1-pcDNA3, IRF3-pcDNA3 or IRF7-pcDNA3 at 24 hours after infection of 229E or OC43 (Figure 6). First, the expressions of IRF1, IRF3 and IRF7 were confirmed (Figure 6A) and then the expression levels of the ISGs before infection were analyzed (Supplementary Figure 5). Following infection of 229E or OC43, most antiviral genes we examined (except GBP2 in IRF7-transfected cells infected with 229E and IFIT2 in IRF1-transfected cells infected with OC43) were significantly elevated in cells introduced with IRF1, IRF3 or IRF7 compared to the vector control infected cells (Figures 6B, C). Furthermore, the expression of GBP2, IFIT2, MAP2, STAT2 and IFN- β was higher in IRF3-transfected cells than in IRF1 and/or IRF7 transfected cells in response to 229E infection (Figure 6B). Similarly, GBP2 and STAT2 transcription were induced more in IRF3-transfected cells during OC43 infection (Figure 6C). These

results suggest that IRF3 has the greatest ability to activate antiviral transcription during human coronavirus infection.

Discussion

In this study, we demonstrated an antiviral role of the IFN-IRF axis against human coronavirus infection. We first found that human coronavirus 229E is moderately sensitive to type I and II IFN, while OC43 is not (Figure 1). Infection of both viruses efficiently induced ISGs and activated IRF1, IRF3 and IRF7, suggesting that the antiviral innate response of infected cells is not fully suppressed during infection (Figures 2, 3). Activation of IRFs was also observed during SARS-CoV-2 infection (Figure 3). The loss- and gain-of-function experiments demonstrated that IRF1

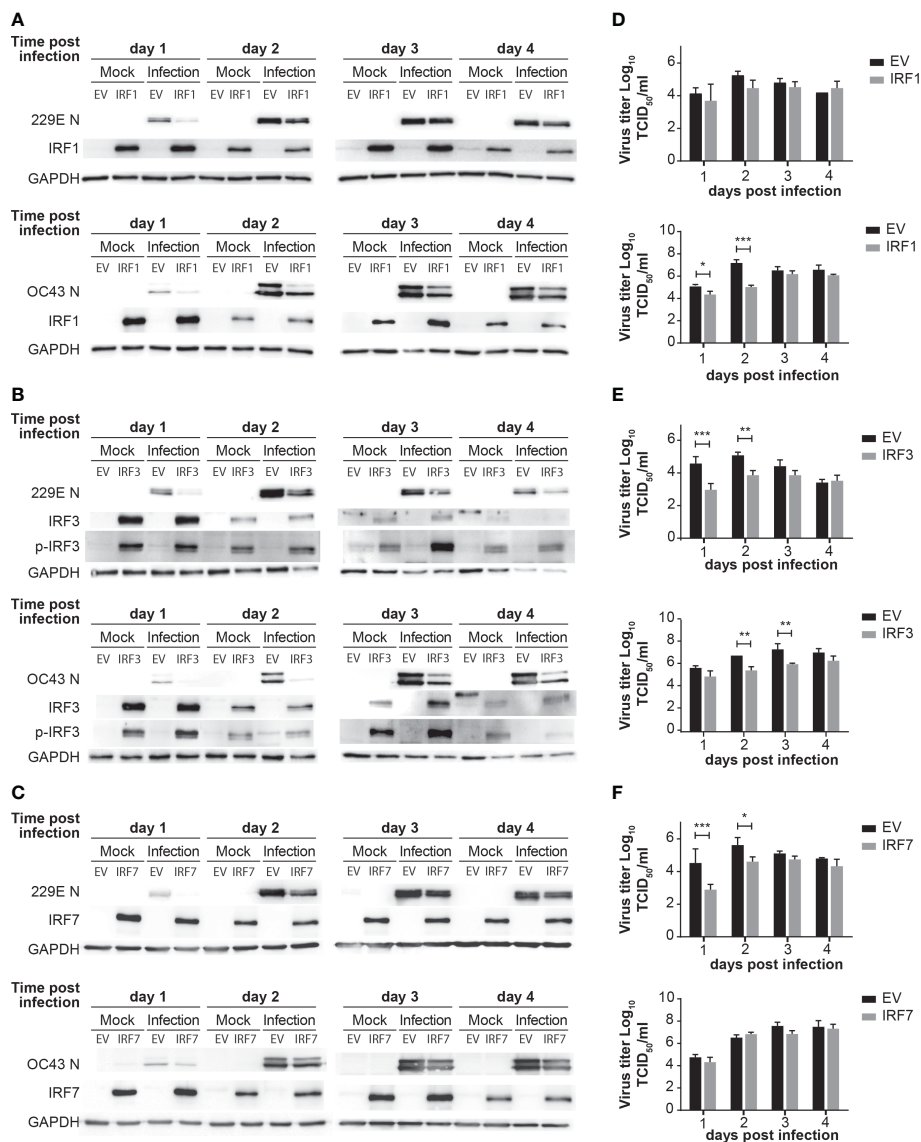


FIGURE 5
Overexpression of IRFs inhibits human coronavirus infection. H1299 cells were transfected with control pcDNA3 empty plasmid (EV) or the plasmid containing IRF1 (A), IRF3 (B) or IRF7 (C) and then infected with or without 229E or OC43 at MOI of 0.01. Virus infection was determined by western blot analysis using antibodies against 229E N protein, OC43 N protein, IRF1, IRF3, IRF7, phosphorylated IRF3 (p-IRF3) and GAPDH. Amounts of progeny viruses were measured in the supernatant of cells transfected with the plasmid containing with IRF1 (D), IRF3 (E) or IRF7 (F) by TCID₅₀ assay which were compared to those transfected with empty plasmid (n=6). *p<0.05, **p<0.01, ***p<0.001, Two-way ANOVA.

and IRF3 have antiviral roles against OC43 infection, while IRF3 and IRF7 were effective in suppressing 229E infection (Figures 4, 5).

We found that 229E is sensitive to type I and II IFN, in agreement with previous studies (20, 27). Type I IFN has been shown to inhibit OC43 infection in A549 (lung cancer cells), yet promotes it in NCI-H520 (lung cancer cells) or Huh 7.5 (hepatoma) (26). In our current study, IFN treatment did not have any effect on OC43 replication in MRC5 (normal fibroblast cells) and H1299 (lung cancer cells). This discrepancy could be due to the differences in cell types. Alternatively, it may be because of IFN concentrations used in this study, which are lower than those used in previous studies. The concentrations of IFN in the present study were based on our previous work on IFN-sensitive viruses (50, 62). A comparison in the same experimental system showed that the

same concentration of IFN completely shuts down the replication of IFN-sensitive VSV, but only partially suppresses 229E while not affecting OC43 (Figures 1F, G). Thus, we conclude that the IFN sensitivity of human coronavirus 229E and OC43 is not very high.

Human coronaviruses are known to inhibit antiviral immunity induced by IFNs at various stages (63, 64). This was also evident in our study as OC43 infection was not sensitive to IFNs (Figure 1; Supplementary Figure 1). However, the ISGs were induced more efficiently in cells infected with OC43 than in those infected with 229E, which is relatively sensitive to IFNs (Figure 2). This may be because OC43 infection does not interfere the ISG induction but may inhibit antiviral effectors involved at later stages of the IFN pathways such as protein kinase R (PKR), the 2',5'-oligoadenylate synthetase (OAS)-RNase L pathway and Mx proteins. Moreover, we

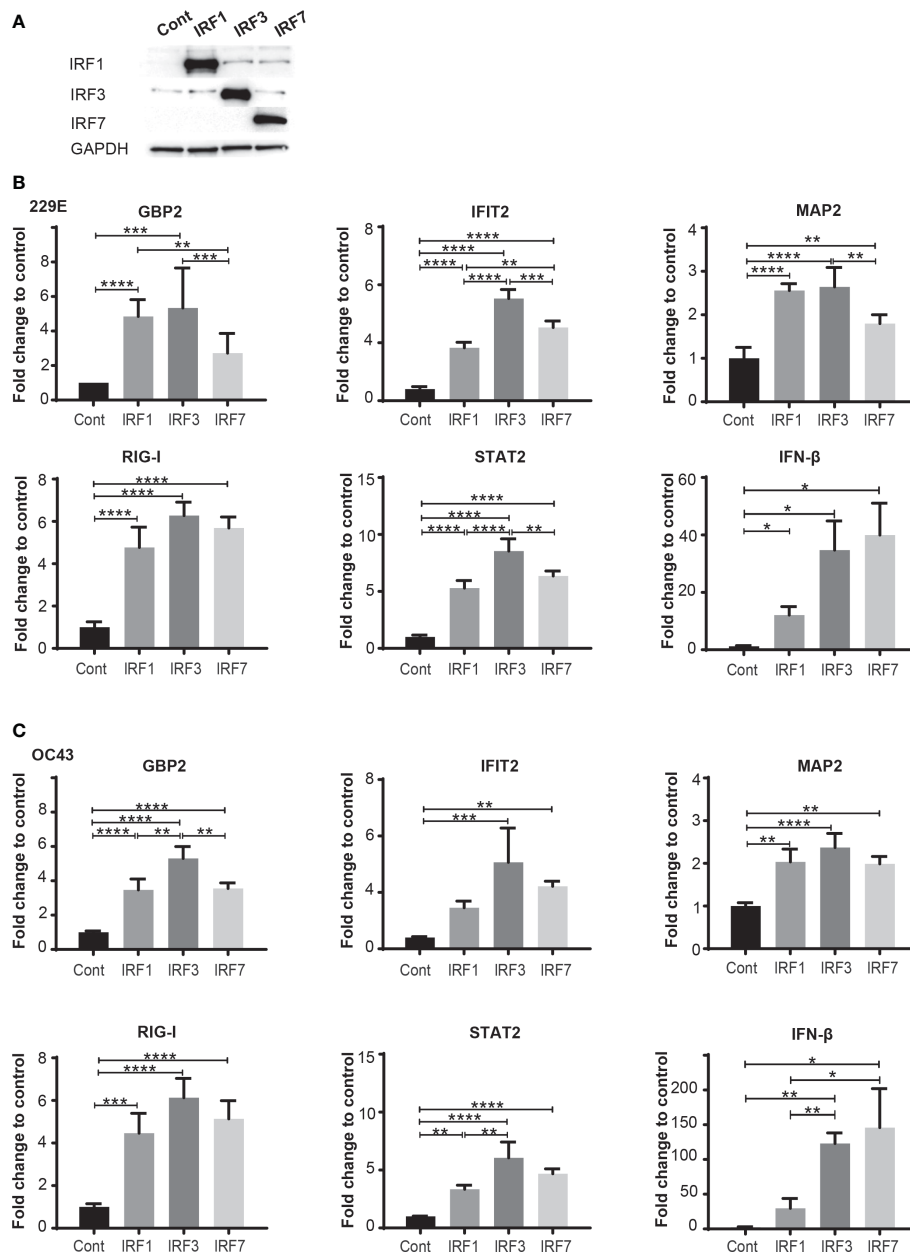


FIGURE 6

IRF3 effectively activates transcription of antiviral genes during human coronavirus infection. H1299 cells were transfected with control pcDNA3 plasmid (Cont) or the plasmid containing IRF1, IRF3 or IRF7 and then infected with or without 229E or OC43 at MOI of 0.01. (A) The expression of IRF1, IRF3 and IRF7 was confirmed by western blot analysis. At 24 hours after infection, the expression of GBP2, IFI2, MAP2, RIG-I, STAT2 and IFN-β in the cells infected with 229E (B) or OC43 (C) was determined by RT-qPCR (n=4). **p<0.01, ***p<0.001, ****p<0.0001, Two-way ANOVA.

Q28

determined the expression levels of 6 selected ISGs among many ISG genes possibly induced during OC43 infection. Therefore, OC43 infection may suppress expression of other ISGs which may play major roles in protecting host cells. Lastly, induction of IFN-inducible transmembrane (IFITM), which is an effective antiviral protein for other viruses, promotes replication of OC43 (26), suggesting that ISG transcription may be required for its efficient replication.

Certain viral proteins of human coronaviruses are known to degrade IRF3 (44, 45). This was the case in our study where the expression of IRF3 was decreased during infection of 229E or OC43

(Figure 3). Nevertheless, we found that IRF3 was efficiently phosphorylated during viral infection (Figure 3). Furthermore, siRNA knockdown of IRF3 increased the susceptibility of host cells to 229E or OC43 infection (Figure 4). These results indicate that IRF3-mediated antiviral response is still active in cells infected with human coronaviruses, although viral evasion downregulates its expression. It was shown previously that BX795, which blocks phosphorylation and translocation of IRF3 (65), inhibits the induction of ISGs and promotes replication of SARS-CoV-2 (43). Considering that IRF3 overexpression inhibited 229E or OC43 infection (Figure 5) and promoted transcription of the antiviral

genes more effectively than IRF1 or IRF7 (Figure 6), IRF3 may be a common antiviral effector against human coronavirus infection, which would make it an excellent antiviral therapeutic target. In contrast, the promotion of IRF1 showed antiviral activities in cells infected with OC43 while IRF7 expression reduced 229E infection (Figure 5). The expression analysis of the antiviral genes did not show the IRF1 and IRF7 bias between 229E and OC43 infection (Figure 6). To answer this, it is essential to further expand our study to investigate antiviral functions of the IRFs using global gene analysis and other human coronaviruses in the future.

IRF1, IRF3 and IRF7 are critical transcriptional regulators of IFNs and ISGs (19, 66, 67). Alternately, IFNs are major transcriptional activators of the IRFs (35). Thus, the activities of IFNs and IRFs are closely related. Interestingly, we found that OC43 is sensitive to antiviral effects of IRF1 and IRF3, but insensitive to IFNs. IRF1 and IRF3 have been reported to have antiviral functions independent of the IFN system, which may be essential to inhibit OC43 infection (41, 42, 68–70). IRF1 and IRF3 upregulate transcription of certain ISGs in IFN-independent manners during virus infection (41, 68–70). Moreover, IRF3 can establish antiviral responses in cells deficient in IFN production (42). Therefore, antiviral functions of IRF1 and IRF3, independent from the IFN system, may be involved in host antiviral responses against OC43 infection. This possibility warrants future investigation.

In our western blot analysis, we observed IRF1 bands, which are higher than expected, at 2 and 3 days after OC43 infection (Figure 3B). Interestingly, this shift was not observed in cells infected with 229E or SARS-CoV-2 infected cells. We believe that the size increase of IRF1 may be due to posttranslational modifications. The phosphorylation or monoubiquitination of IRF1 promotes its transcriptional activity (71). While this may be the reason why IRF1 showed antiviral activities against OC43 infection but not 229E infection (Figure 5A), it is yet to be clarified why they were observed only in cells infected with OC43.

We use MRC5 cells for most of our studies (Figures 1–4), but H1299 cells were used for the gain-of-function experiments for IRFs (Figure 5). This is because we encountered technical problems achieving sufficient expression levels of IRFs without causing cell morbidity or affecting virus infection in MRC5 cells during transfection.

Q18 Data availability statement

The original contributions presented in the study are included in the article/Supplementary Materials. Further inquiries can be directed to the corresponding author.

Q20 Author contributions

DX: conducted siRNA knockdown, infection of the viruses, western blot analysis and RT-qPCR analysis, and involved in manuscript preparation. JD: Conducted overexpression of IRFs, infection of the viruses and western blot analysis, and involved in manuscript preparation. ML: Conducted TCID₅₀ assay, infection of

viruses and western blot analysis, and involved in manuscript preparation. JG: Conducted SARS-CoV-2 infection. YK: Established SARS-CoV-2 infection system and supervised the project. KH: Supervised the project, designed the experiments, and completed the manuscript. All authors contributed to the article and approved the submitted version.

Acknowledgments

This work was supported by grants from the Canadian Institutes for Health Research (CIHR) (KH), the Natural Sciences and Engineering Research Council of Canada (NSERC) (KH), the Japan Agency for Medical Research and Development (AMED) (Grant Number JP20wm0125002) (YK and JG), a grant from the international Joint Research Project of the Institute of Medical Science, the University of Tokyo and Memorial University of Newfoundland (KH). DX was supported by the Dean's fellowship from Faculty of Medicine, Memorial University of Newfoundland. Special thanks to Dr. Yoshihiro Kawaoka (Division of Virology, Department of Microbiology and Immunology, Institute of Medical Science, University of Tokyo) for SARS-CoV-2 samples and Dr. John Bell (University of Ottawa, Ottawa, Canada) for providing VSV. Dr. Jessica Esseltine (Memorial University of Newfoundland) for a culture system of human dermal fibroblast cells.

Conflict of interest

The authors declare that the research was conducted in the absence of any commercial or financial relationships that could be construed as a potential conflict of interest.

Publisher's note

All claims expressed in this article are solely those of the authors and do not necessarily represent those of their affiliated organizations, or those of the publisher, the editors and the reviewers. Any product that may be evaluated in this article, or claim that may be made by its manufacturer, is not guaranteed or endorsed by the publisher.

Supplementary material

The Supplementary Material for this article can be found online at: <https://www.frontiersin.org/articles/10.3389/fimmu.2023.930086/full#supplementary-material>

SUPPLEMENTARY FIGURE 1

H1299 cells were left untreated or treated with IFN- α or IFN- γ , for 16 hours prior to infection (IFN prior to infection) or from 16 hours prior to infection to Day 6 (IFN whole period). The cells were challenged with 229E or OC43 infection at MOI of 0.01. (A) Western blot analysis of viral protein was conducted using anti 229E N protein, OC43 N protein and GAPDH antibodies. (B) TCID₅₀ assay was performed to measure the progeny virus

of 229E or OC43 at 6 days post infection. * $p < 0.05$, ** $p < 0.01$, *** $p < 0.001$, Two-way ANOVA.

SUPPLEMENTARY FIGURE 2

(A) MRC5 cells were left untreated or stimulated with IFN- α (500 U/ml) or IFN- γ (100 U/ml) for 16 hours. (B, C) MRC5 cells were left uninfected or infected with UV-inactivated 229E (B) or UV-inactivated OC43 (C) at MOI of 0.01 for 2 and 4 days. The expression levels of ISG mRNA (GBP2, RIG-I and STAT2) were determined by RT-qPCR. The relative quantification (RQ) indicates the fold change of the expression level for infected samples towards that of the non-infected controls at the same time point post infection. The transcriptional level for each gene was calculated by normalizing to GAPDH expression level and then normalized by the corresponding control. * $p < 0.05$, ** $p < 0.01$, *** $p < 0.001$, **** $p < 0.0001$, Two-way ANOVA.

SUPPLEMENTARY FIGURE 3

(A) MRC5 cells were left untreated or stimulated with IFN- α (500 U/ml) or IFN- γ (100 U/ml) for 8, 16, 24 and 48 hours. (B, C) MRC5 cells were left uninfected or infected with UV-inactivated 229E (B) or UV-inactivated OC43

(C) at MOI of 0.01 for 2 and 4 days. The activation of IRF1, 3 and 7 was determined by western blot analysis using antibodies against 229E N protein, OC43 N protein, IRF1, IRF3, IRF7, phosphorylated (p-IRF3) and GAPDH.

SUPPLEMENTARY FIGURE 4

Human dermal fibroblasts were left uninfected (-) or infected (+) with 229E (A) or OC43 (B) at MOI of 0.01. The activation of IRF1, IRF3 and IRF7 was determined by western blot analysis using antibodies against 229E N protein, OC43 N protein, IRF1, IRF3, IRF7, phosphorylated (p-IRF3) and GAPDH.

SUPPLEMENTARY FIGURE 5

H1299 cells were transfected with control pcDNA3 plasmid (Cont) or the plasmid containing IRF1, IRF3 or IRF7. At 24 hours after transfection, the expression of GBP2, IFI2, MAP2, RIG-I, STAT2 and IFN- β was determined by RT-qPCR (n=4). * $p < 0.05$, ** $p < 0.01$, *** $p < 0.001$, **** $p < 0.0001$, Two-way ANOVA.

SUPPLEMENTARY TABLE 1

Sequence of qPCR primers.

References

1. Sturman LS, Holmes KV. The molecular biology of coronaviruses. *Adv Virus Res* (1983) 28:35–112. doi: 10.1016/S0065-3527(08)60721-6
2. Wege H, Siddell S, ter Meulen V. The biology and pathogenesis of coronaviruses. *Curr Top Microbiol Immunol* (1982) 99:165–200. doi: 10.1007/978-3-642-68528-6_5
3. Seddiq N, Al-Qahtani M, Al-Tawfiq JA, Bukamal N. First confirmed case of middle East respiratory syndrome coronavirus infection in the kingdom of Bahrain: In a Saudi gentleman after cardiac bypass surgery. *Case Rep Infect Dis* (2017) 2017:1262838. doi: 10.1155/2017/1262838
4. Su S, Wong G, Shi W, Liu J, Lai ACK, Zhou J, et al. Epidemiology, genetic recombination, and pathogenesis of coronaviruses. *Trends Microbiol* (2016) 24(6):490–502. doi: 10.1016/j.tim.2016.03.003
5. LIVE C. COVID-19 coronavirus pandemic (2022). Available at: <https://www.worldometers.info/coronavirus/>.
6. Corman VM, Muth D, Niemeyer D, Drosten C. Hosts and sources of endemic human coronaviruses. *Adv Virus Res* (2018) 100:163–88. doi: 10.1016/bs.aivir.2018.01.001
7. Dominguez SR, Shrivastava S, Berglund A, Qian Z, Goes LGB, Halpin RA, et al. Isolation, propagation, genome analysis and epidemiology of HKU1 betacoronaviruses. *J Gen Virol* (2014) 95(Pt 4):836–48. doi: 10.1099/vir.0.059832-0
8. van der Hoek L, Pyrc K, Jebbink MF, Vermeulen-Oost W, Berkhout RJ, Wolthers KC, et al. Identification of a new human coronavirus. *Nat Med* (2004) 10(4):368–73. doi: 10.1038/nm1024
9. Brian DA, Baric RS. Coronavirus genome structure and replication. *Curr Top Microbiol Immunol* (2005) 287:1–30. doi: 10.1007/3-540-26765-4_1
10. Davies JP, Almsay KM, McDonald EF, Plate L. Comparative multiplexed interactomics of SARS-CoV-2 and homologous coronavirus nonstructural proteins identifies unique and shared host-cell dependencies. *ACS Infect Dis* (2020) 6(12):3174–89. doi: 10.1021/acinfecdis.0c00500
11. Schlee M, Hartmann G. Discriminating self from non-self in nucleic acid sensing. *Nat Rev Immunol* (2016) 16(9):566–80. doi: 10.1038/nri.2016.78
12. Iwanaszko M, Kimmel M. NF-kappaB and IRF pathways: cross-regulation on target genes promoter level. *BMC Genomics* (2015) 16:307. doi: 10.1186/s12864-015-1511-7
13. Servant MJ, Tenover B, Lin R. Overlapping and distinct mechanisms regulating IRF-3 and IRF-7 function. *J Interferon Cytokine Res* (2002) 22(1):49–58. doi: 10.1089/107999002753452656
14. Yan N, Chen ZJ. Intrinsic antiviral immunity. *Nat Immunol* (2012) 13(3):214–22. doi: 10.1038/nri.2229
15. McNab F, Mayer-Barber K, Sher A, Wack A, O'Garra A. Type I interferons in infectious disease. *Nat Rev Immunol* (2015) 15(2):87–103. doi: 10.1038/nri3787
16. Ivashkiv LB, Donlin LT. Regulation of type I interferon responses. *Nat Rev Immunol* (2014) 14(1):36–49. doi: 10.1038/nri3581
17. Platanias LC. Mechanisms of type-I- and type-II-interferon-mediated signalling. *Nat Rev Immunol* (2005) 5(5):375–86. doi: 10.1038/nri1604
18. Au-Yeung N, Mandhana R, Horvath CM. Transcriptional regulation by STAT1 and STAT2 in the interferon JAK-STAT pathway. *JAKSTAT*. (2013) 2(3):e23931. doi: 10.4161/jkst.23931
19. Feng H, Zhang YB, Gui JF, Lemon SM, Yamane D. Interferon regulatory factor 1 (IRF1) and anti-pathogen innate immune responses. *PLoS Pathog* (2021) 17(1): e1009220. doi: 10.1371/journal.ppat.1009220
20. Kindler E, Jonsdottir HR, Muth D, Hamming OJ, Hartmann R, Rodriguez R, et al. Efficient replication of the novel human betacoronavirus EMC on primary human epithelium highlights its zoonotic potential. *mBio*. (2013) 4(1):e00611–12. doi: 10.1128/mBio.00611-12
21. Rai MK, Upadhyay SK, Agrawal SC. *In vitro* evaluation of three topical antimicrobials against ring-worm fungi singly and in combination. *Hindustan Antibiot Bull* (1992) 34(3-4):104–7. Q23
22. Stroher U, DiCaro A, Li Y, Strong JE, Aoki F, Plummer F, et al. Severe acute respiratory syndrome-related coronavirus is inhibited by interferon- α . *J Infect Dis* (2004) 189(7):1164–7. doi: 10.1086/382597
23. Zielecki F, Weber M, Eickmann M, Spiegelberg L, Zaki AM, Matrosovich M, et al. Human cell tropism and innate immune system interactions of human respiratory coronavirus EMC compared to those of severe acute respiratory syndrome coronavirus. *J Virol* (2013) 87(9):5300–4. doi: 10.1128/JVI.03496-12
24. Clementi N, Ferrarese R, Crisculo E, Diotti RA, Castelli M, Scagnolari C, et al. Interferon-beta-1a inhibition of severe acute respiratory syndrome-coronavirus 2 *In vitro* when administered after virus infection. *J Infect Dis* (2020) 222(5):722–5. doi: 10.1093/infdis/jiaa350
25. Lokugamage KG, Hage A, de Vries M, Valero-Jimenez AM, Schindewolf C, Dittmann M, et al. Type I interferon susceptibility distinguishes SARS-CoV-2 from SARS-CoV. *J Virol* (2020) 94(23). doi: 10.1128/JVI.01410-20 Q22
26. Zhao X, Guo F, Liu F, Cuconati A, Chang J, Block TM, et al. Interferon induction of IFITM proteins promotes infection by human coronavirus OC43. *Proc Natl Acad Sci U S A*. (2014) 111(18):6756–61. doi: 10.1073/pnas.1320856111
27. Sperber SJ, Hayden FG. Comparative susceptibility of respiratory viruses to recombinant interferons-alpha 2b and -beta. *J Interferon Res* (1989) 9(3):285–93. doi: 10.1089/jir.1989.9.285
28. Davoudi-Monfared E, Rahmani H, Khalili H, Hajiabdolbaghi M, Salehi M, Abbasian L, et al. A randomized clinical trial of the efficacy and safety of interferon beta-1a in treatment of severe COVID-19. *Antimicrob Agents Chemother* (2020) 64(9). doi: 10.1128/AAC.01061-20
29. Haagmans BL, Kuiken T, Martina BE, Fouchier RA, Rimmelzwaan GF, van Amerongen G, et al. Pegylated interferon-alpha protects type 1 pneumocytes against SARS coronavirus infection in macaques. *Nat Med* (2004) 10(3):290–3. doi: 10.1038/nm1001
30. Frieman MB, Chen J, Morrison TE, Whitmore A, Funkhouser W, Ward JM, et al. SARS-CoV pathogenesis is regulated by a STAT1 dependent but a type I, II and III interferon receptor independent mechanism. *PLoS Pathog* (2010) 6(4):e1000849. doi: 10.1371/journal.ppat.1000849
31. Channappanavar R, Fehr AR, Vijay R, Mack M, Zhao J, Meyerholz DK, et al. Dysregulated type I interferon and inflammatory monocyte-macrophage responses cause lethal pneumonia in SARS-CoV-infected mice. *Cell Host Microbe* (2016) 19(2):181–93. doi: 10.1016/j.chom.2016.01.007
32. Blanco-Melo D, Nilsson-Payant BE, Liu WC, Uhl S, Hoagland D, Moller R, et al. Imbalanced host response to SARS-CoV-2 drives development of COVID-19. *Cell*. (2020) 181(5):1036–45 e9. doi: 10.1016/j.cell.2020.04.026

- 1345 33. Ji L, Wang N, Ma J, Cheng Y, Wang H, Sun J, et al. Porcine deltacoronavirus
1346 nucleocapsid protein species-specifically suppressed IRF7-induced type I interferon
1347 production via ubiquitin-proteasomal degradation pathway. *Vet Microbiol* (2020)
250:108853. doi: 10.1016/j.vetmic.2020.108853
- 1348 34. Taniguchi T, Ogasawara K, Takaoka A, Tanaka N. IRF family of transcription
1349 factors as regulators of host defense. *Annu Rev Immunol* (2001) 19:623–55. doi:
10.1146/annurev.immunol.19.1.623
- 1350 35. Nguyen H, Hiscott J, Pitha PM. The growing family of interferon regulatory
1351 factors. *Cytokine Growth Factor Rev* (1997) 8(4):293–312. doi: 10.1016/S1359-6101(97)
00019-1
- 1352 36. Fujita T, Kimura Y, Miyamoto M, Barsoumian EL, Taniguchi T. Induction of
1353 endogenous IFN- α and IFN- β genes by a regulatory transcription factor, IRF-1.
1354 *Nature*. (1989) 337(6204):270–2. doi: 10.1038/337270a0
- 1355 37. Savitsky D, Tamura T, Yanai H, Taniguchi T. Regulation of immunity and
1356 oncogenesis by the IRF transcription factor family. *Cancer Immunol Immunother.*
1357 (2010) 59(4):489–510. doi: 10.1007/s00262-009-0804-6
- 1358 38. Schoggins JW, Wilson SJ, Panis M, Murphy MY, Jones CT, Bieniasz P, et al. A
1359 diverse range of gene products are effectors of the type I interferon antiviral response.
1360 *Nature*. (2011) 472(7344):481–5. doi: 10.1038/nature09907
- 1361 39. Chen HW, King K, Tu J, Sanchez M, Luster AD, Shrestha S. The roles of IRF-3
1362 and IRF-7 in innate antiviral immunity against dengue virus. *J Immunol* (2013) 191
1363 (8):4194–201. doi: 10.4049/jimmunol.1300799
- 1364 40. Wang P, Zhao W, Zhao K, Zhang L, Gao C. TRIM26 negatively regulates
1365 interferon- β production and antiviral response through polyubiquitination and
1366 degradation of nuclear IRF3. *PLoS Pathog* (2015) 11(3):e1004726.
- 1367 41. Ashley CL, Abendroth A, McSharry BP, Slobedman B. Interferon-independent
1368 upregulation of interferon-stimulated genes during human cytomegalovirus infection is
1369 dependent on IRF3 expression. *Viruses*. (2019) 11(3). doi: 10.3390/v11030246
- 1370 42. Chew T, Noyce R, Collins SE, Hancock MH, Mossman KL. Characterization of
1371 the interferon regulatory factor 3-mediated antiviral response in a cell line deficient for
1372 IFN production. *Mol Immunol* (2009) 46(3):393–9. doi: 10.1016/j.molimm.2008.10.010
- 1373 43. Cheemarla NR, Watkins TA, Mihaylova VT, Wang B, Zhao D, Wang G, et al.
1374 Dynamic innate immune response determines susceptibility to SARS-CoV-2 infection
1375 and early replication kinetics. *J Exp Med* (2021) 218(8). doi: 10.1084/jem.20210583
- 1376 44. Moustaqil M, Ollivier E, Chiu HP, Van Tol S, Rudolff-Soto P, Stevens C, et al.
1377 SARS-CoV-2 proteases PLpro and 3CLpro cleave IRF3 and critical modulators of
1378 inflammatory pathways (NLRP12 and TAB1): implications for disease presentation
1379 across species. *Emerg Microbes Infect* (2021) 10(1):178–95. doi: 10.1080/
22221751.2020.1870414
- 1380 45. Zhang W, Ma Z, Wu Y, Shi X, Zhang Y, Zhang M, et al. SARS-CoV-2 3C-like
1381 protease antagonizes interferon- β production by facilitating the degradation of IRF3.
1382 *Cytokine*. (2021) 148:155697. doi: 10.1016/j.cyto.2021.155697
- 1383 46. Kouwaki T, Nishimura T, Wang G, Oshiumi H. RIG-I-Like receptor-mediated
1384 recognition of viral genomic RNA of severe acute respiratory syndrome coronavirus-2
1385 and viral escape from the host innate immune responses. *Front Immunol* (2021)
1386 12:700926. doi: 10.3389/fimmu.2021.700926
- 1387 47. Sui L, Zhao Y, Wang W, Wu P, Wang Z, Yu Y, et al. SARS-CoV-2 membrane
1388 protein inhibits type I interferon production through ubiquitin-mediated degradation
1389 of TBK1. *Front Immunol* (2021) 12:662989. doi: 10.3389/fimmu.2021.662989
- 1390 48. Kawamoto S, Oritani K, Asada H, Takahashi I, Ishikawa J, Yoshida H, et al.
1391 Antiviral activity of limitin against encephalomyocarditis virus, herpes simplex virus,
1392 and mouse hepatitis virus: diverse requirements by limitin and alpha interferon for
1393 interferon regulatory factor 1. *J Virol* (2003) 77(17):9622–31. doi: 10.1128/
1394 JVI.77.17.9622-9631.2003
- 1395 49. Li S, Zhu Z, Yang F, Cao W, Yang J, Ma C, et al. Porcine epidemic diarrhea virus
1396 membrane protein interacted with IRF7 to inhibit type I IFN production during viral
1397 infection. *J Immunol* (2021) 206(12):2909–23. doi: 10.4049/jimmunol.2001186
- 1398 50. Battcock SM, Collier TW, Zu D, Hirasawa K. Negative regulation of the alpha
1399 interferon-induced antiviral response by the Ras/Raf/MEK pathway. *J Virol* (2006) 80
1400 (9):4422–30. doi: 10.1128/JVI.80.9.4422-4430.2006
- 1401 51. Gary EN, Warner BM, Parzych EM, Griffin BD, Zhu X, Taylor N, et al. A novel
1402 mouse AAV6 hACE2 transduction model of wild-type SARS-CoV-2 infection studied
1403 using synDNA immunogens. *iScience*. (2021) 24(7):102699. doi: 10.1016/
1404 j.isci.2021.102699
- 1405 52. Camargo C, Lupien A, McIntosh F, Menzies D, Behr MA, Sagan SM.
1406 Effectiveness of germicidal ultraviolet light to inactivate coronaviruses on personal
1407 protective equipment to reduce nosocomial transmission. *Infect Control Hosp
1408 Epidemiol.* (2022) 43(7):886–91. doi: 10.1017/ice.2021.249
- 1409 53. Bucknall RA, King LM, Kapikian AZ, Chanock RM. Studies with human
1410 coronaviruses. II. some properties of strains 229E and OC43. *Proc Soc Exp Biol Med*
1411 (1972) 139(3):722–7. doi: 10.3181/00379727-139-36224
- 1412 54. Christian SL, Zu D, Licursi M, Komatsu Y, Pongnopparat T, Codner DA, et al.
1413 Suppression of IFN-induced transcription underlies IFN defects generated by activated
1414 Ras/MEK in human cancer cells. *PLoS One* (2012) 7(9):e44267. doi: 10.1371/
1415 journal.pone.0044267
- 1416 55. Hou W, Wang X, Ye L, Zhou L, Yang ZQ, Riedel E, et al. Lambda interferon
1417 inhibits human immunodeficiency virus type 1 infection of macrophages. *J Virol* (2009)
1418 83(8):3834–42. doi: 10.1128/JVI.01773-08
- 1419 56. Stoltz M, Klingstrom J. Alpha/beta interferon (IFN- α /beta)-independent
1420 induction of IFN- λ 1 (interleukin-29) in response to hantavirus infection. *J
1421 Virol* (2010) 84(18):9140–8. doi: 10.1128/JVI.00717-10
- 1422 57. Briken V, Ruffner H, Schultz U, Schwarz A, Reis LF, Strehlow I, et al. Interferon
1423 regulatory factor 1 is required for mouse gbp gene activation by gamma interferon. *Mol
1424 Cell Biol* (1995) 15(2):975–82. doi: 10.1128/MCB.15.2.975
- 1425 58. Kitamura A, Takahashi K, Okajima A, Kitamura N. Induction of the human
1426 gene for p44, a hepatitis-c-associated microtubular aggregate protein, by interferon-
1427 alpha/beta. *Eur J Biochem* (1994) 224(3):877–83. doi: 10.1111/j.1432-
1428 1033.1994.00877.x
- 1429 59. Bluysen HA, Vlietstra RJ, van der Made A, Trapman J. The interferon-
1430 stimulated gene 54 K promoter contains two adjacent functional interferon-
1431 stimulated response elements of different strength, which act synergistically for
1432 maximal interferon- α inducibility. *Eur J Biochem* (1994) 220(2):395–402. doi:
1433 10.1111/j.1432-1033.1994.tb18636.x
- 1434 60. Yoneyama M, Kikuchi M, Natsukawa T, Shinobu N, Imaizumi T, Miyagishi M,
1435 et al. The RNA helicase RIG-I has an essential function in double-stranded RNA-
1436 induced innate antiviral responses. *Nat Immunol* (2004) 5(7):730–7. doi: 10.1038/
1437 ni1087
- 1438 61. Improta T, Schindler C, Horvath CM, Kerr IM, Stark GR, Darnell JE Jr.
1439 Transcription factor ISGF-3 formation requires phosphorylated Stat91 protein, but
1440 Stat113 protein is phosphorylated independently of Stat91 protein *Proc Natl Acad Sci U
1441 S A.* (1994) 91(11):4776–80
- 1442 62. Komatsu Y, Derwish L, Hirasawa K. IRF1 downregulation by Ras/MEK is
1443 independent of translational control of IRF1 mRNA. *PLoS One* (2016) 11(8):e0160529.
1444 doi: 10.1371/journal.pone.0160529
- 1445 63. Minkoff JM, tenOever B. Innate immune evasion strategies of SARS-CoV-2. *Nat
1446 Rev Microbiol* (2023) 21(3):178–94. doi: 10.1038/s41579-022-00839-1
- 1447 64. Park A, Iwasaki A. Type I and type III interferons - induction, signaling, evasion,
1448 and application to combat COVID-19. *Cell Host Microbe* (2020) 27(6):870–8. doi:
1449 10.1016/j.chom.2020.05.008
- 1450 65. Clark K, Plater L, Peggie M, Cohen P. Use of the pharmacological inhibitor
1451 BX795 to study the regulation and physiological roles of TBK1 and IkappaB kinase
1452 epsilon: a distinct upstream kinase mediates ser-172 phosphorylation and activation. *J
1453 Biol Chem* (2009) 284(21):14136–46. doi: 10.1074/jbc.M109.000414
- 1454 66. Petro TM. IFN regulatory factor 3 in health and disease. *J Immunol* (2020) 205
1455 (8):1981–9. doi: 10.4049/jimmunol.2000462
- 1456 67. Ning S, Pagano JS, Barber GN. IRF7: activation, regulation, modification and
1457 function. *Genes Immun* (2011) 12(6):399–414. doi: 10.1038/gene.2011.21
- 1458 68. Xiang C, Yang Z, Xiong T, Wang T, Yang J, Huang M, et al. Avian IRF1 and
1459 IRF7 play overlapping and distinct roles in regulating IFN-dependent and
1460 -independent antiviral responses to duck tembusu virus infection. *Viruses* (2022) 14
1461 (7). doi: 10.3390/v14071506
- 1462 69. Irving AT, Zhang Q, Kong PS, Luko K, Rozario P, Wen M, et al. Interferon
1463 regulatory factors IRF1 and IRF7 directly regulate gene expression in bats in response
1464 to viral infection. *Cell Rep* (2020) 33(5):108345. doi: 10.1016/j.celrep.2020.108345
- 1465 70. Hare DN, Baid K, Dvorkin-Gheva A, Mossman KL. Virus-intrinsic differences
1466 and heterogeneous IRF3 activation influence IFN-independent antiviral protection.
1467 *iScience*. (2020) 23(12):101864.
- 1468 71. Garvin AJ, Khalaf AHA, Rettino A, Xicluna J, Butler L, Morris JR, et al.
1469 GSK3 β -SCFFBX7 α mediated phosphorylation and ubiquitination of IRF1
1470 are required for its transcription-dependent turnover. *Nucleic Acids Res* (2019) 47
1471 (9):4476–94. doi: 10.1093/nar/gkz163

Joint Seminar in Virology

March 9 (Thu) 2023, @IMSUT First Building, Auditorium

- 13:00-13:05 Opening Remarks
Yasushi KAWAGUCHI (Professor, IMSUT)
- 13:05-13:35 Ken HIRASAWA (Professor, MUN)
“Why are cancers more susceptible to virus infection?”
- 13:35-14:05 Akihisa KATO (Associate Professor, IMSUT)
“A novel HSV-1 evasion mechanism for a glia-specific restriction factor and its role in viral encephalitis“
- 14:05-14:30 Maria LICURSI (Post-doctoral fellow, MUN)
“Antiviral roles of IRF1, IRF3 and IRF7 in response to human coronavirus infection”
- 14:30-14:55 Kosuke TAKESHIMA (Research Associate, IMSUT)
“Role of lamin A/C and lamin B receptor in viral replication of herpes simplex virus type 1”
- 14:55-15:15 Break
- 15:15-15:35 Lingyan WANG (PhD student, MUN)
“Promotion of human coronavirus infection by programmed cell death”
- 15:35-15:55 Ayano FUKUI (PhD student, IMSUT)
“Dual impacts of a glycan shield on the envelope glycoprotein B of HSV-1: Evasion from human antibodies in vivo and neurovirulence”
- 15:55-16:15 Joseph DUNCAN (PhD student, MUN)
“Roles of extracellular vesicles during human coronavirus infection”
- 16:15-16:35 Moeka NOBE (PhD student, IMSUT)
“Direct relationship between protein expression and progeny yield of herpes simplex virus 1 unveils a rate-limiting step for virus production”
- 16:35-16:45 Noah CONOHAN (MSc student, MUN)
“Sensitivity of RNA viruses to antiviral functions of the heme pathway”
- 16:45-16:50 Closing Remarks
Ken HIRASAWA (Professor, MUN)